Molecular Crystals and Liquid Crystals

Publication details, including instructions for authors and subscription information:
http://www.tandfonline.com/loi/gmcl20

Self-Assembly and Photoisomerizationof Azobenzenealkanethiol Derivativeson Gold Films: Infrared Reflection Absorption Studies

T. Sato [a], K. Tsuji [a], E. Kokuryu [a], T. Wadayama [a] & A. Hatta [a]

[a] Department of Materials Science, Graduate Schoolof Engineering, Tohoku University, Aoba-yama 02, Sendai, 980-8579, Japan

Version of record first published: 18 Oct 2010

To cite this article: T. Sato, K. Tsuji, E. Kokuryu, T. Wadayama & A. Hatta (2002): Self-Assembly and Photoisomerizationof Azobenzenealkanethiol Derivativeson Gold Films: Infrared Reflection Absorption Studies, Molecular Crystals and Liquid Crystals, 391:1, 13-39

To link to this article: http://dx.doi.org/10.1080/10587250216173

Mol. Cryst. Liq. Cryst., Vol. 391, pp. 13–39

1542-1406/03 $12.00 + .00
DOI: 10.1080/15421400390193558

Taylor & Francis
Taylor & Francis Group

SELF-ASSEMBLY AND PHOTOISOMERIZATION OF AZOBENZENEALKANETHIOL DERIVATIVES ON GOLD FILMS: INFRARED REFLECTION ABSORPTION STUDIES

*T. Sato, K. Tsuji, E. Kokuryu, T. Wadayama, and A. Hatta**
Department of Materials Science, Graduate School of Engineering, Tohoku University, Aoba-yama 02, Sendai 980-8579, Japan

Self-assembly and photoisomerization of 4-(4′-(phenylazo) phenoxy) undecane-1-thiol and its fluoro- and methoxy-phenylazo derivatives on evaporated gold films have been characterized by infrared reflection absorption spectroscopy. The infrared measurements as a function of self-assembling time show that their self-assembling proceeds through Langmuir adsorption with a settlement in alignment of the azobenzene moiety and the aliphatic long chain. Moreover, photoisomerizations of these compounds from trans *to* cis *and vice versa are very limited in their close-packed monolayer films in contrast to the molecules in solution. However, such restrictions are somewhat relaxed for a self-assembly film of the* cis*-form methoxy-phenylazo derivative. This effect of preferential* cis*-form assembling is also demonstrated by the changes in the alignment of 4-cyano-4′-pentylbiphenyl (5CB) nematic liquid crystalline molecules caused by conformational changes of the underlying self-assembled molecules.*

Keywords: photoisomerization; infrared spectroscopy; self-assembly; liquid crystal; molecular alignment

INTRODUCTION

The chemistry of the so-called self-assembled monolayer (SAM) has attracted much attention from both basic and applied viewpoints. Representative molecules forming SAMs on gold are alkanethiols with a terminal S-H bond. They form rigid structures on gold surfaces via dehydrogenated chemisorption and van der Waals forces between the SAM molecules. SAMs can be taken as a new class of materials that can be used for technologies

Received 2 July 2002; accepted 22 October 2002.
*Corresponding author. Fax: 81-22-217-7318, E-mail-hatta@ material.tohoku.ac.jp

including photoresists, biosensors, microcontact printing, etc., as noted in the literature [1]. SAMs can be formed not only on gold but also on copper and silver. Of particular interest is the study the influences of these substrates on the structure and the orderliness of SAMs formed by chemisorption of thiol compounds. Actually, Laibinis et al. [2] and Laibinis and Whitesides [3] have successfully conducted X-ray photoelectron spectroscopy (XPS) as well as infrared reflection absorption spectroscopy (IRRAS) to investigate the structures of SAMs prepared from various alkanetiols ($HS(CH_2)_nR$) on gold, copper, and silver surfaces. A subject of particular interest from an applied standpoint is the SAMs of photosensitive geometrical isomers since their structures are possible to change from one to another. These bistable states can function as optical switch elements.

By means of ultraviolet-visible (UV-visible) absorption spectroscopy, Ichimura et al. [4–7,9] and Maak et al. [8] have shown that the alignment of liquid crystal (LC) molecules can be controlled by photoisomerizations of the underlying azobenzene derivatives. This is primarily due to intermolecular interactions between LC and photochemical molecules. Surprisingly, however, little work of this kind has been performed to date with IRRAS, which has already been established as a convenient means for high-sensitive detection and identification of adsorbed molecules on metal surfaces [10–13]. In the present work, IRRAS is used to characterize the self-assembling and photoisomerization of azobenzenealkanethiol derivatives on vacuum-evaporated gold films. In addition, we investigate the alignments of nematic LC molecules on the self-assembled azobenzenealkanethiols before and after photoisomerization.

EXPERIMENTAL

4-(4′-(phenylazo)phenoxy)undecane-1-thiol and fluoro- and methoxyphenylazo derivatives (hereafter abbreviated as AZO11, F-AZO11, and M-AZO11, respectively) were used as self-assembling molecules. These compounds (*trans*-rich) were purchased from Hayashibara Biochemical Institute Co. and used without further purification. Chemical structures of these compounds are shown in Figure 1. These thiol compounds were allowed to self-assembled on gold films 200 nm thick deposited by electron-beam evaporation onto quartz plates. The gold-deposited quartz plates were immersed for 24 h at maximum into chloroform solutions containing 1×10^{-3} M thiol compounds. The SAM films thus prepared were rinsed with chloroform and subsequently ethanol, and then dried in air. The IRRAS spectra of these SAM films were taken on a Fourier transform infrared (FTIR) spectrometer (Bomen, MB100) with p-polarized radiation incident at an angle of 80° from the metal surface normal as a function of immersion

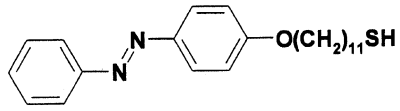

4-(4'-(phenylazo)phenoxy)undecane-1-thiol (**AZO11**)

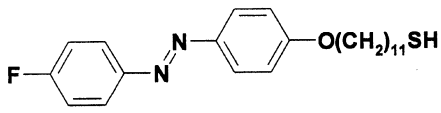

4-(4'-(fluorophenylazo)phenoxy)undecane-1-thiol (**F-Azo11**)

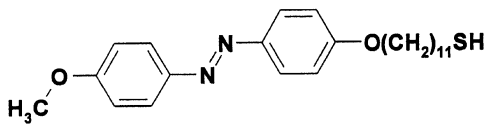

4-(4'-(methoxyphenylazo)phenoxy)undecane-1-thiol (**M-Azo11**)

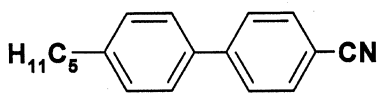

4-cyano-4'-pentylbiphenyl (**5CB**)

FIGURE 1 Chemical structures of AZO11, F-AZO11, M-AZO11, and 5CB.

time and also of UV or visible light irradiation time. Each of the IRRAS spectra was divided by the background spectrum measured before SAM formation. The spectra were obtained as the average of 128 scans at 4 cm^{-1} resolution.

UV-visible spectra were measured for the thiol compounds in chloroform solutions in the region 300–600 nm with a diode array spectrophotometer (Hamamatsu Photonics, PMA11) equipped with an optical fiber to guide radiation to the detector. The light source was a 150 W Xe lamp.

For *trans*-to-*cis* photoisomerization of the SAMs, UV radiation ($\lambda \leqq$ 365 nm) from a high-pressure Hg lamp (100 W) was irradiated through a visible-cut filter (Hoya, U340), whereas for *cis*-to-*trans* photoisomerization visible radiation ($\lambda \geqq 437$ nm) from the Hg lamp was irradiated through a UV-cut filter (Toshiba Glass, L42).

The nematic liquid crystal, 4-cyano-4′-pentylbiphenyl (5CB), was obtained from Chisso Chemicals Co. The chemical structure of 5CB is shown in Figure 1. An approximately 100 nm thick 5CB film was deposited from its chloroform solution onto each of the SAMs to compare the alignments of 5CB molecules before and after photoisomerization of the SAMs.

RESULTS AND DISCUSSION

Vibrational Assignments for AZO11 Compounds

First of all, infrared transmission spectra of *trans*-form AZO11, F-AZO11, and M-AXO11 were obtained in the KBr pellets. Because these spectra resembled each other, we only show the spectrum of *trans* F-AZO11 in Figure 2. The bands at 2917 and 2850 cm^{-1} can be assigned to the asymmetric and symmetric stretch modes of the long chain CH_2 groups. A very weak band due to S-H stretching is located at 2550 cm^{-1}. The bands at

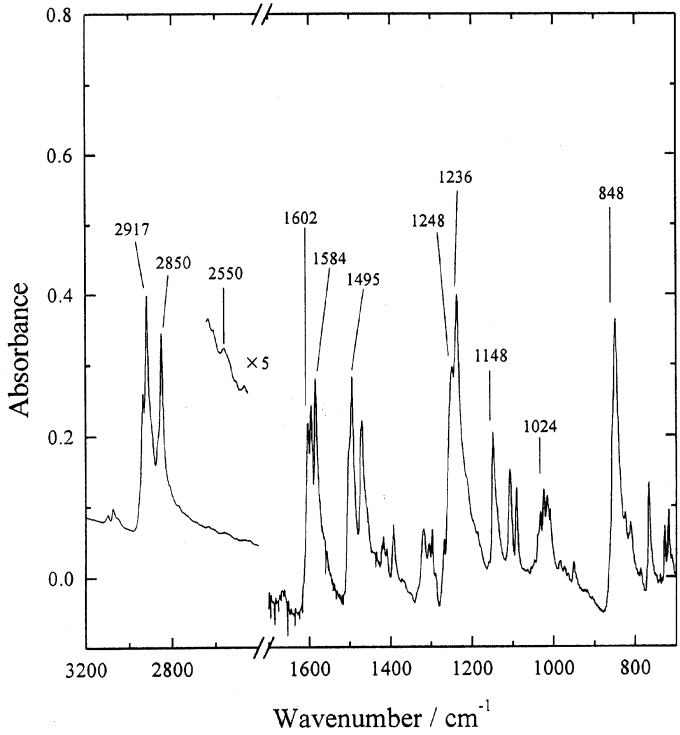

FIGURE 2 Infrared absorption spectrum of *trans* F-AZO11 in KBr disk.

1602, 1584, and 1495 cm^{-1} are all ascribable to phenyl stretching vibrations. The bands at 1248 (shoulder) and 1236 cm^{-1} are assigned to the phenyl-O-C asymmetric and phenyl-F stretching modes, respectively. The 1148 cm^{-1} band is ascribed to phenyl-N stretch vibrations and the 1024 cm^{-1} band to the phenyl-O-C symmetric stretch. The band at 848 cm^{-1} is due to the in-phase out-of-plane phenyl hydrogen wagging vibration. Obviously, almost all of these assignments are applicable to *trans*-form AZO11 and M-AZO11. On the basis of the normal dipole selection rule operative in IRRAS [14], these vibrational assignments will be confirmed by the IRRAS spectra of the SAMs investigated in the present work.

Photoisomerization of AZO11 Compounds in Chloroform

UV-visible absorption measurements were carried out to confirm the photoisomerization of AZO11 compounds in a conventional manner. The differences in UV-visible absorption between *trans* and *cis* forms of azobenzene are well known [15]. Figure 3 shows the UV-visible spectra of a chloroform solution containing 5×10^{-5} M F-AZO11 (*trans*-rich), measured under UV ($\lambda \leqq 365$ nm) irradiation (left) and subsequently under visible ($\lambda \geqq 437$ nm) irradiation (right). Accordingly, these spectra refer to *trans*-to-*cis* and *cis*-to-*trans* photoisomerizations in sequence. The irradiation time-dependence of the band intensities observed in each photoisomerization process is principally due to a diffusion of the molecules between the dark and illuminated regions in the solution. The intense absorption band observed at 347 nm before UV irradiation is attributed to the $\pi \rightarrow \pi^*$ transition of *trans*-form F-AZO11. This band decreases in intensity and shifts to 333 nm after 10 min of UV irradiation as a result of *trans*-to-*cis* isomerization. The weak absorption band at 442 nm arises from the $n \rightarrow \pi^*$ transition of either *trans* or *cis* isomer; this band increases in intensity with increasing UV irradiation time in conformity with the fact that for azobenzene the absorption coefficient of $n \rightarrow \pi^*$ transition is larger in the *cis* form than in the *trans* form. It is clear from the spectra (right) in Figure 3 that subsequent visible irradiation ($\lambda \geqq 437$ nm) produces *trans*-form F-AZO11. Essentially the same spectral changes were observed for AZO11. The situation is a little different for M-AZO11; the *trans* form showed $n \rightarrow \pi^*$ and $\pi \rightarrow \pi^*$ transition bands at 450 and 358 nm, respectively, and additionally the latter band exhibited no blue shift in the *trans*-to-*cis* isomerization process, though an additional absorption feature was observed at 320 nm as shoulder of the $\pi \rightarrow \pi^*$ transition band.

Self-Assembly of *trans* AZO11 Compounds

In order to investigate the self-assembling behavior of *trans* F-AZO11 on gold, IRRAS spectra were measured as a function of assembling time during

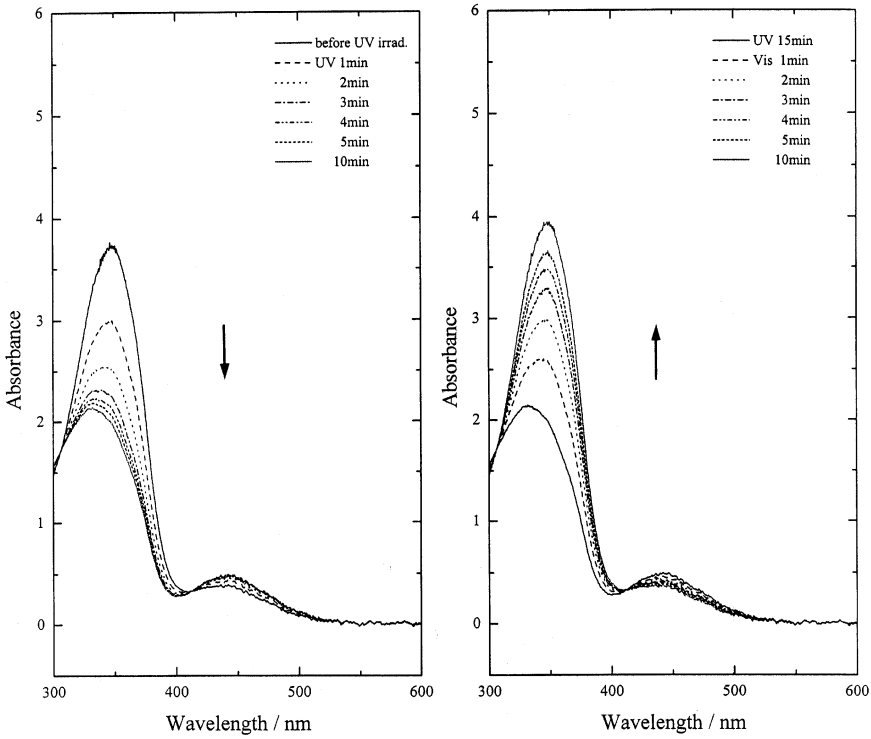

FIGURE 3 UV-visible spectral changes of *trans* F-AZO11 in chloroform with increasing UV irradiation time (left) and visible irradiation time (right) in succession.

which a gold-deposited quartz plate was immersed in 1×10^{-3} M F-AZO11 solution. The spectra observed in the region from 2000 to 800 cm^{-1} are shown in Figure 4. The IRRAS bands of the self-assembly films appear at nearly the same frequencies as those in the transmission spectrum of *trans* F-AZO11 shown in Figure 2. However, differences in relative intensities are noticed between any of the self-assembly films and the F-AZO11 crystals in KBr matrix. According to the surface selection rule of IRRAS [14], only modes of vibrations that yield a dynamical dipole moment (transition moment) perpendicular to the surface should be observed strongly. On the other hand, the molecules in the KBr matrix are aligned at random as a whole. Therefore, the differences in the relative band intensities can be interpreted in terms of a molecular alignment in the self-assembled film.

Figure 5 depicts a conformational model for *trans* F-AZO11 before self-assembling. This model was obtained by use of a semiempirical molecular

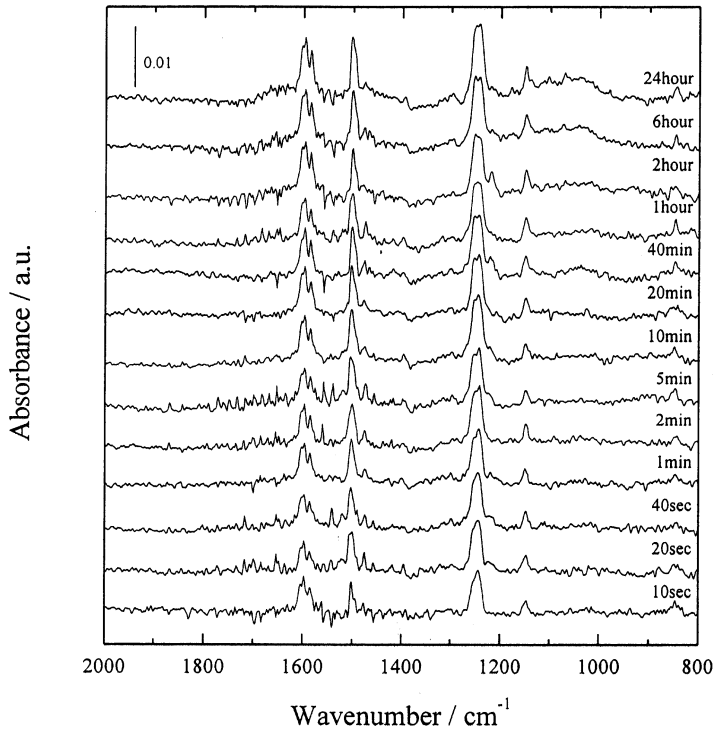

FIGURE 4 IRRAS spectra of *trans* F-AZO11 self-assembled from chloroform solution onto evaporated gold, taken as a function increasing assembling time.

orbital calculation program (MOPAC) under the assumption that the aliphatic chain extends in a *trans* zigzag conformation. We also calculated the angle (β) between the molecular long axis and the transition moment for each vibration mode. The values of β for some selected modes are given in the inset of Figure 5. It is found that the phenyl-O-C asymmetric stretch mode has a transition moment approximately parallel to the molecular long axis, whereas that of the phenyl-O-C symmetric stretch as well as of the phenyl out-of-plane hydrogen wagging points nearly perpendicular to the long axis. Accordingly, the strong intensity of the phenyl-O-C a symmetric stretch band in comparison to the phenyl-O-C symmetric stretch and phenyl out-of-plane hydrogen wagging bands (Figure 4) can be explained in terms of an anisotropy of the SAM in which the long axes of the molecules are aligned perpendicular rather than parallel to the gold surface.

Figure 6 illustrates the variations with increasing immersion time of the absorbance values of the phenyl-O-C asymmetric stretch (1252 cm^{-1}),

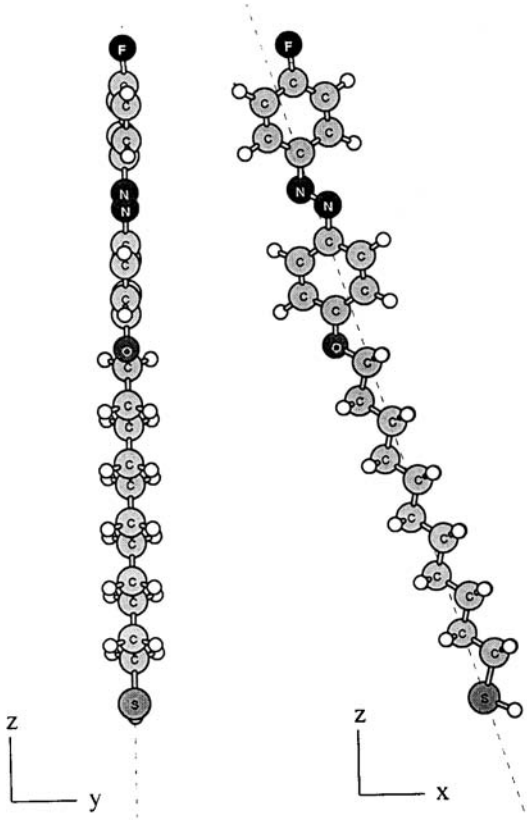

Vibrational modes	β (degrees)
$\nu_{as}(CH_2)$	85.5
$\nu_{s}(CH_2)$	89.9
ν_{as}(ph-O-C)	13.1
ν (ph-F)	13.1
ν (ph-N)	17.4
ν_{s}(ph-O-C)	79.2
δ (C-H)	88.3

FIGURE 5 Molecular conformation of *trans* F-AZO11 derived by MOPAC calculations. In the inset calculated values of β, i.e., the angle between the transition moment direction and the long axis of the molecule, are give for the indicated vibration modes.

phenyl-F stretch (1244 cm^{-1}), and phenyl-N stretch bands (1149 cm^{-1}) for self-assembled *trans* F-AZO11. It is immediately clear that any band at first rapidly increases in intensity and continues to increase at a much slower rate, followed by reaching a maximum. This is the very feature that is expected for the formation of a single molecular layer *via* self-regulating adsorption (Langmuir type). Nearly the same features were observed in the self-assembling of *trans* AZO11 and M-AZO11, as shown in Figures 7 and 8, respectively. The saturation behaviors shown in Figures 6–8 demonstrate that in any case the self-assembling is almost completed after 6 h of immersion. It is worthwhile to compare the assembling behaviors of

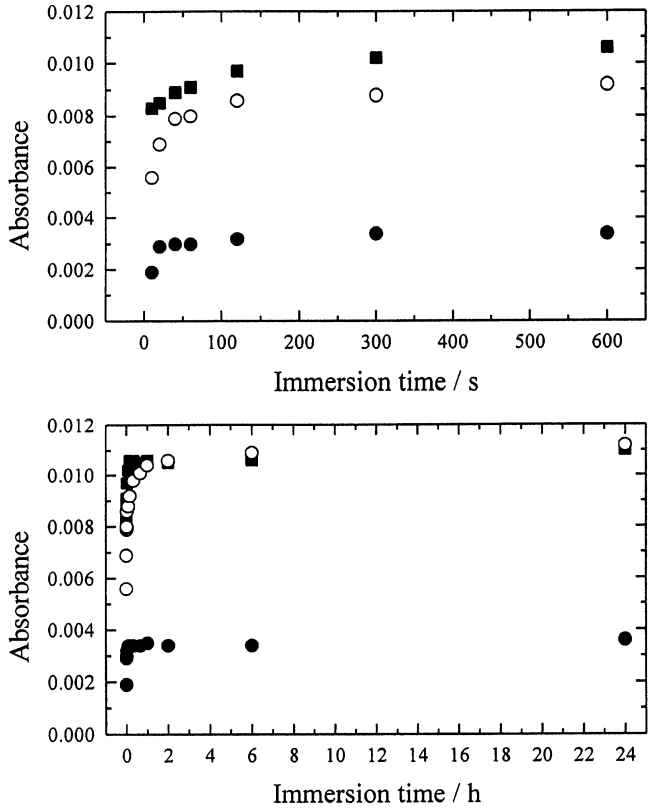

FIGURE 6 Absorbance values for the phenyl-O-C asymmetric stretch (○), phenyl-F stretch (■), and phenyl-N stretch (●) modes of *trans* F-AZO11 SAM versus assembling (immersion) time.

trans F-AZO11, AZO11, and M-AZO11 in more detail. Looking closely, one may notice that the intensity variations at the early stages of self-assembling are different between the phenyl-N stretch and phenyl-O-C asymmetric stretch bands. The largest difference is seen in the AZO11 self-assembling where the former band saturates more rapidly than the latter band. This indicates that the alignment of the azobenzene moieties precedes the alignment of the aliphatic chains. This is not the case for the assembling of M-AZO11, where no remarkable difference is observed between the phenyl-N and phenyl-O-C asymmetric stretch bands, and hence participation of the large terminal O-CH_3 group is suggested. Thus, it is clear that the size of the terminal group exerts influence on the self-assembling of these compounds.

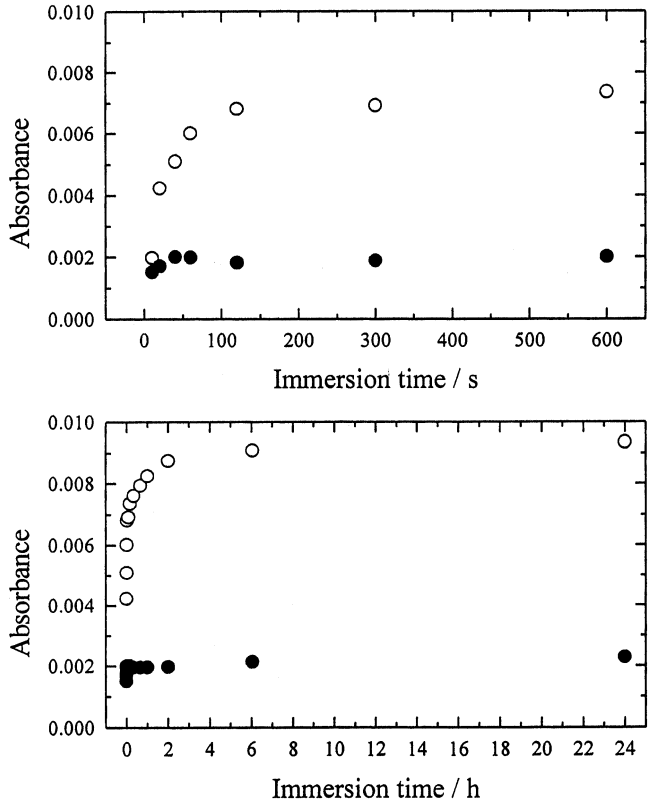

FIGURE 7 The same as in Figure 6, but for the phenyl-O-C asymmetric stretch (○) and phenyl-N stretch (●) modes of *trans* AZO11 SAM.

Since self-assembling in general proceeds through chemisorption, atomically flat surfaces with suitable interatomic distances would favor the formation a close-packed self-assembly monolayer (SAM) structure. Actually, Caldwell et al. [16] characterized the SAM of *trans* AZO11 on Au(111) based on atomic force microscopy and X-ray diffraction measurements and proposed a bundle model to explain the close packing of the azobenzene groups in a hexagonal lattice. Attainment of this SAM structure is undoubtedly due to suitable arrangements of the surface gold atoms. Of course, such a close packing of the molecules cannot be expected in the present work, where the substrates are evaporated gold films (polycrystalline) which inevitably have no uniform atomic structures and should provide a variety of adsorption sites. It is easily supposed that *trans*-to-*cis* isomerization is hardly possible for such a close-packed SAM of AZO11 on Au(111).

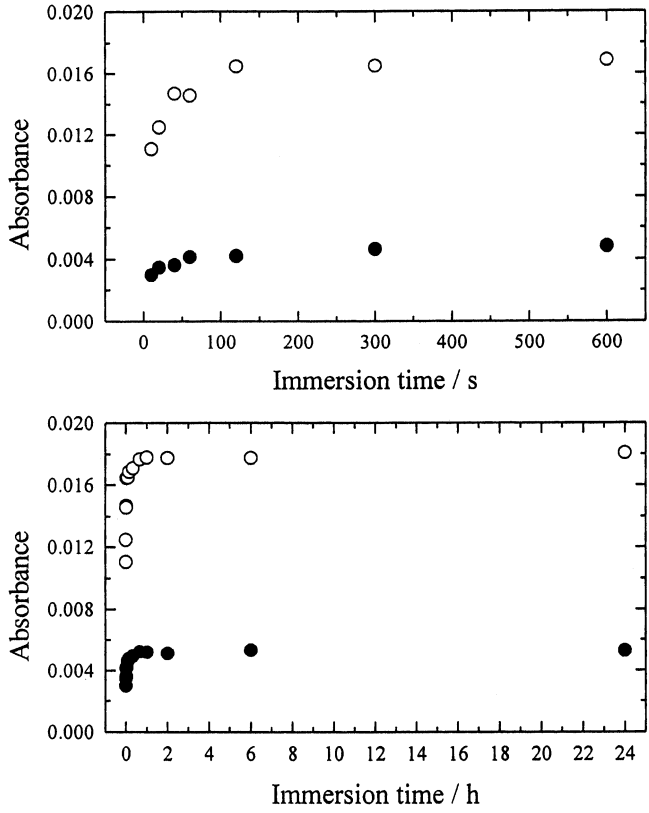

FIGURE 8 The same as in Figure 6, but for the phenyl-O-C asymmetric stretch (○) and phenyl-N stretch (●) modes of *trans* M-AZO11's SAM.

Photoisomerization of Self-Assembled *trans* AZO11 Derivatives

Our separate UV-visible measurements revealed that *trans*-to-*cis* photoisomerization is suppressed for the SAMs of AZO11 derivatives on gold films. The same conclusion was drawn from IRRAS spectral measurements for self-assembled *trans*-form AZO11 derivatives under irradiation of UV, visible, and UV in sequence. For the sake of space, we present here the results for the *trans*-form SAMs of F-AZO11 and M-AZO11. The samples were prepared by immersing gold films in chloroform solution for 24 h. The IRRAS spectral changes of the F-AZZO11's SAM caused by irradiation of UV, visible, and UV in sequence are shown in Figure 9, where (a), (b), and (c) are the sequential spectra, and (d) and (e) are difference spectra (b)–(a) and (c)–(b), respectively. At first glance the phenyl-O-C

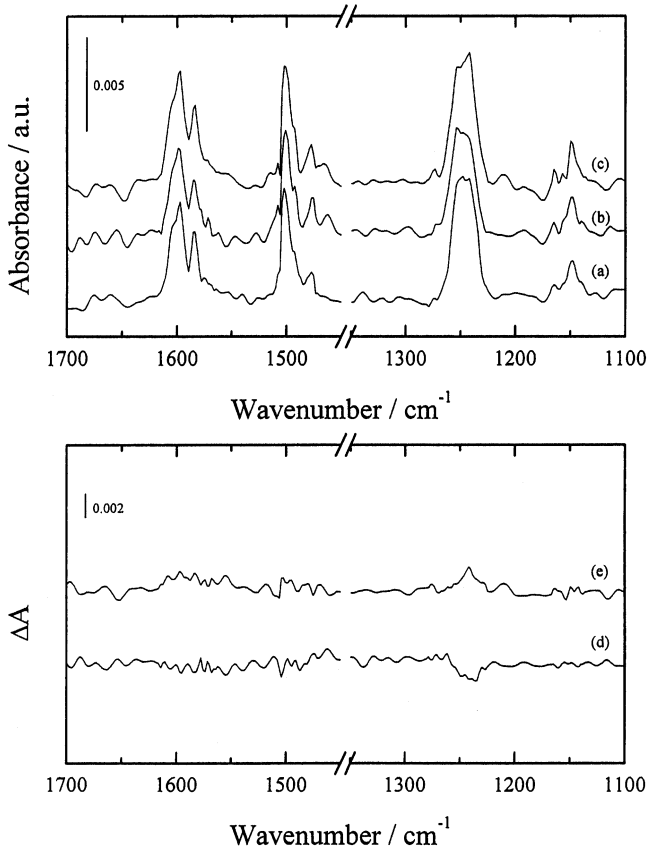

FIGURE 9 IRRAS spectral changes of *trans* AZO11 self-assembled on gold: (a) before UV irradiation, (b) after UV irradiation (20 min), (c) after visible irradiation (20 min) in sequence, (d) difference spectrum (b)–(a), and (e) difference spectrum (c)–(b).

asymmetric stretch ($1254\,cm^{-1}$) as well as the phenyl-F stretch ($1244\,cm^{-1}$) appears to decrease in intensity by UV irradiation and increase by subsequent visible irradiation. However, from the difference in spectra shown in Figure 9, we judge the former band to hardly change in intensity. This also fits in our MOPAC conformation models: in the *trans* form the upper phenyl-N group is coplanar with the lower phenyl-N group, whereas in the *cis* form the upper part is twisted and bent with respect to the lower one without change in the alignment of the phenyl-O-C moiety. Accordingly, the phenyl-F moiety in the *trans* form is directed perpendicular rather than parallel to the gold surface, but the reverse is true in the

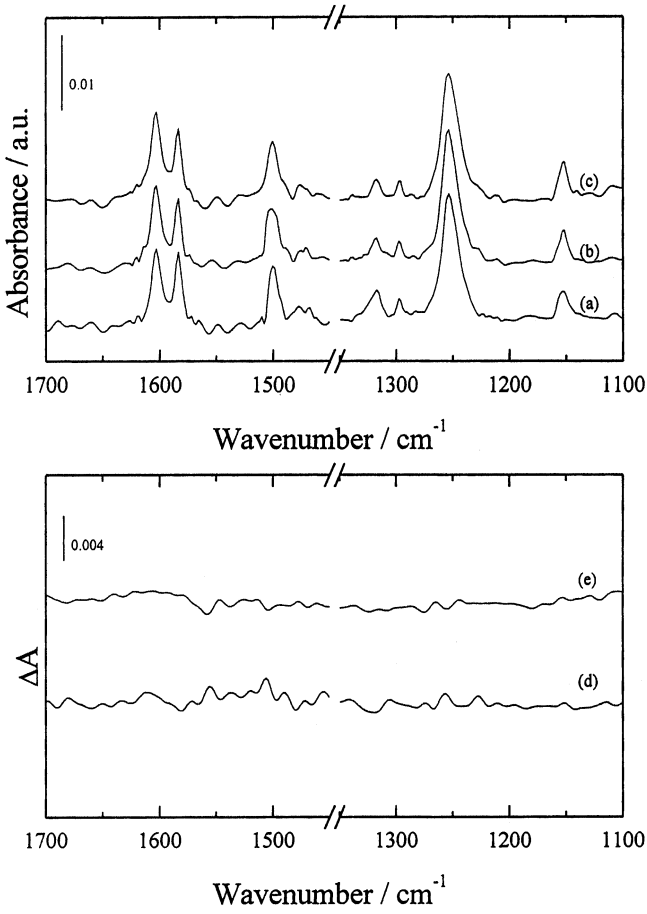

FIGURE 10 The same as in Figure 9, but for *trans* M-AZO11.

cis form. Indeed the phenyl-F stretch band is most intense in the difference spectra shown in Figure 9. As is evident from its intensity in (d), however, the *trans*-to-*cis* isomerization efficiency is very limited in contrast to that in solution shown in Figure 3, suggesting the requirement of larger space for that isomerization to take place in the F-AZO11's SAM. Nevertheless, it must be pointed out that the *trans-cis* isomerization did occur, though only partially. This may probably be associated with the polycrystalline substrate that consists predominantly of high-index facets. Surface roughness and other imperfections may also be relevant to the attainment of the partial isomerization.

Figure 10 shows the corresponding IRRAS results for the SAM of M-AZO11. In this case no significant difference can be seen between difference spectra (e) and (d). This is primarily due to lack of pertinent vibrations that can distinguish between *trans* and *cis* forms. However, a possible candidate for this purpose is the phenyl-O-CH_3 asymmetric stretch that has not been described. This band appears near 1250 cm^{-1} as will become clear later, and it is indistinguishable in position from the phenyl-O-C asymmetric stretch band. However, like the phenyl-F stretch this band should be more sensitive to isomerization than the phenyl-O-C asymmetric band. We believe the failure to observe this band definitely in (d) and (e) of Figure 10 indicates that photoisomerization is more limited in the SAM of M-AZO11 than that in the F-AZO11's SAM. This undoubtedly must be attributed to the large O-CH_3 headgroup.

Photoisomerization of Self-Assembled *cis* AZO11 Derivatives

In view of the limited photoisomerization for the *trans*-form SAMs mentioned above, we also examined the case where the *cis* molecules were assembled in expectation of more isomerization efficiency. Figures 11 and 12 depict the IRRAS spectral changes of F-AZO11 and M-AZO11 SAMs, respectively, upon irradiation of visible, UV, and visible in sequence. The original samples were prepared under UV irradiation for 24 h. The spectral changes due to *cis*-to-*trans* isomerization and subsequent *trans*-to-*cis* isomerization are shown in difference spectra (d) and (e) of these figures. It is found that the change in intensity of the phenyl-F stretch band by *cis*-to-*trans* isomerization is essentially the same as the change caused by *cis* isomerization of the *trans*-form SAM shown in (d) of Figure 9. However, the situation is rather different for the *cis*-form SAM of M-AZO11, as described below.

It is found from Figure 12 that, in addition to the phenyl-ring stretch bands in the 1600 cm^{-1} region, an absorption feature appears near 1250 cm^{-1} as positive in (d) and as negative in (e). As described before, this feature is ascribed not to the phenyl-O-C asymmetric stretch but to the phenyl-O-CH_3 asymmetric stretch, though the former band is also located near 1250 cm^{-1}. The transition moment of the phenyl-O-CH_3 asymmetric mode lies approximately parallel to the upper phenyl group, and its intensity should be more intense in a *trans* form than in a *cis* form. Obviously, the same description is possible for the phenyl-ring stretch bands observed in Figure 12. It should be noted that the phenyl-O-CH_3 asymmetric stretch is not definitely observed in the difference spectra shown in Figure 10. The same is also true for the phenyl-ring stretch bands, although they are observed as rather intensified in (d) and (e) of Figure 12.

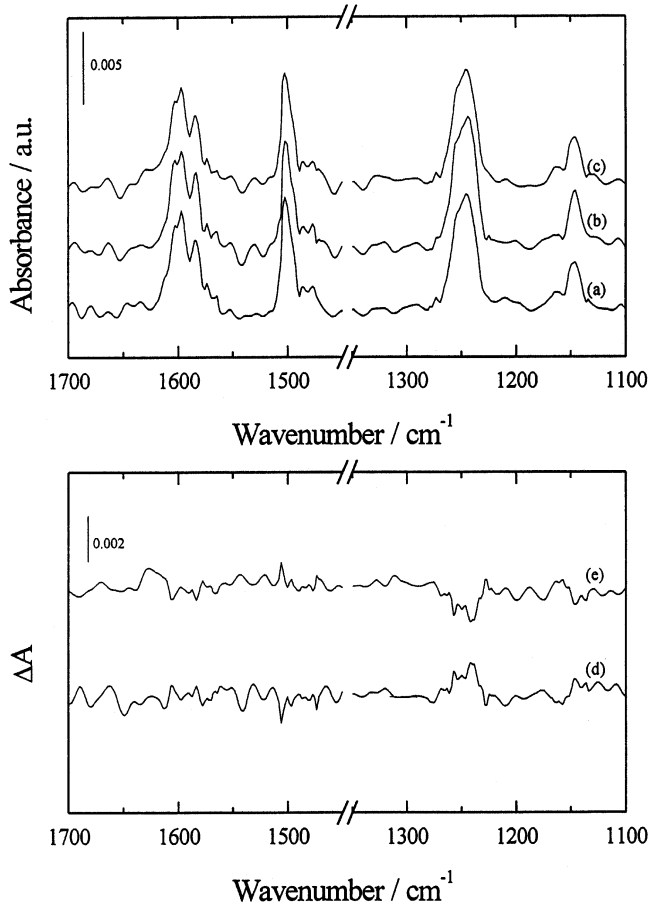

FIGURE 11 IRRAS spectral changes for *cis* F-AZO11 self-assembled on gold: (a) before visible irradiation, (b) after visible irradiation (20 min), (c) after UV irradiation (20 min) in sequence, (d) difference spectrum (b)–(a), and (e) difference spectrum (c)–(b).

The enhancement of the phenyl-ring bands as well as the phenyl-O-CH_3 band shows that initial self-assembling of a *cis* SAM is preferable for M-AZO11, in particular from a viewpoint of the photoisomerization efficiency. In other words, the effect of *cis*-SAM formation in the beginning is larger for larger molecular cross section. In what follows, this effect will be demonstrated on the basis of the alignment of 5CB molecules deposited on the SAMs of AZO11 compounds.

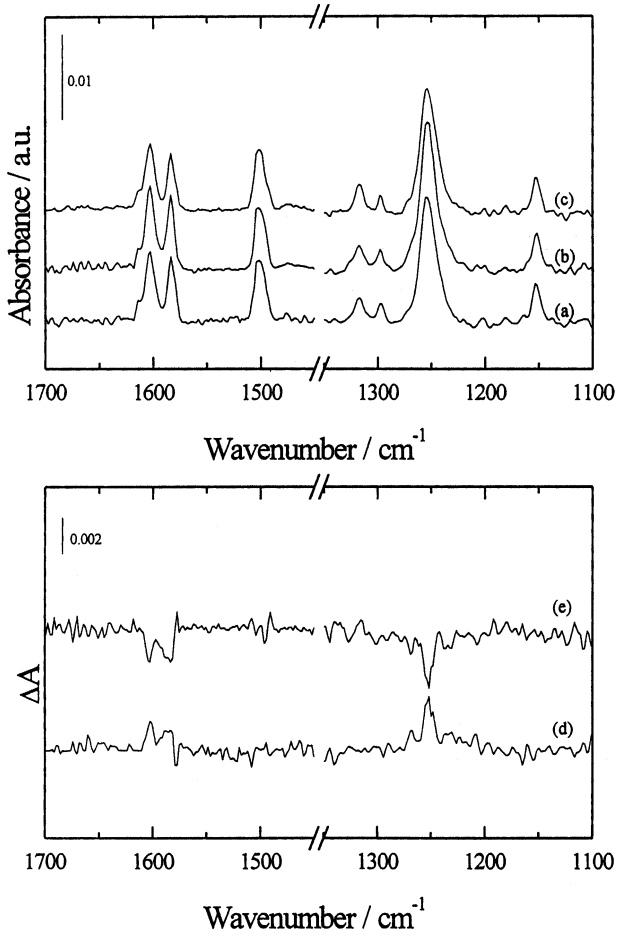

FIGURE 12 The same as in Figure 11, but for *cis* M-AZO11.

Interfacial Interactions Between 5CB Liquid Crystal and SAMs of *trans* AZO11 Derivatives

We also used IRRAS to investigate the molecular alignment of nematic 5CB molecules on the SAMs of *trans* AZO11 derivatives as self-assembled from chloroform solution on gold films. Here we focus on their effect of photo-isomerization upon a change in the alignment of the LC molecules. 5CB molecules assume a nematic phase in the range 24–35°C and turn into an isotropic phase above 35°C. Nematic molecules in general tend to align uniaxially with their long molecular axes parallel to some common direction

(preferred direction). Interactions between the LC molecules and the substrate surface play a primary role in determining the LC alignment. The surface-induced alignment can spread quite far from the substrate surface (i.e., several tens of micrometers or more) in spite of relatively weak intermolecular interactions. In the following we discuss the alignment of nematic 5CB molecules deposited as a thickness of 100 nm by reference to that observed in the isotropic phase.

The IRRAS spectra of 5CB films on the SAMs of F-AZO11 and M-AXO11 are shown in Figures 13 and 14, respectively. In both figures (a) through (c) refer to the LC layer just after formation at 25°C, the isotropic LC layer at 45°C, and the nematic layer cooled down to 25°C, respectively. The bands at 2928 and 2857 cm^{-1} are due to the CH_2 asymmetric and symmetric stretch modes, respectively. The 2226 cm^{-1} band is attributed to the CN stretch (ν_{CN}), and the 1606 and 1494 cm^{-1} bands are attributed to the phenyl-ring modes, which primarily involve C-C stretch vibrations (ν_{CC}). The bands lying close together at 829 and 812 cm^{-1} can be assigned to the in-phase out-of-plane hydrogen wagging vibrations (δ_{CH}). Our MOPAC calculations as well as polarized infrared ATR measurements of nematic

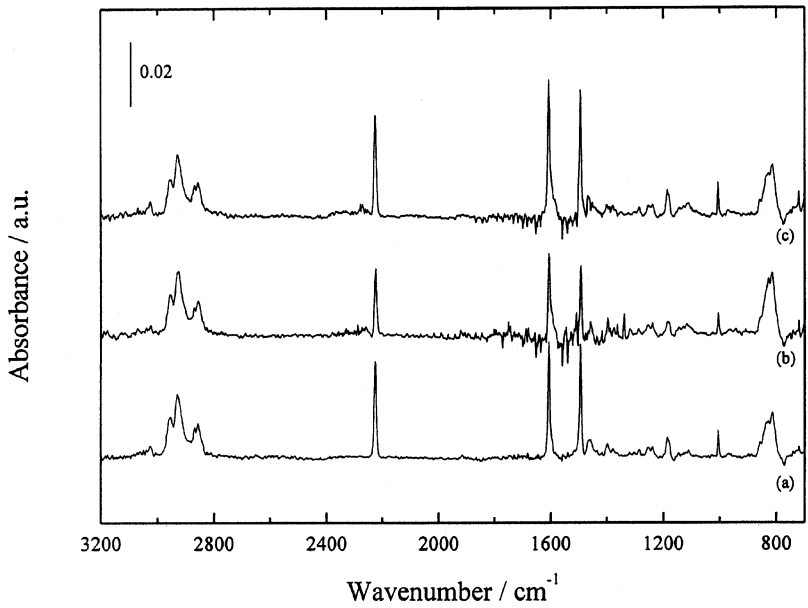

FIGURE 13 IRRAS spectra of 100 nm thick 5CB deposited on self-assembled *trans* F-AZO11: (a) just after deposition at 25°C, (b) isotropic phase at 45°C, and (c) after cooling down to 25°C.

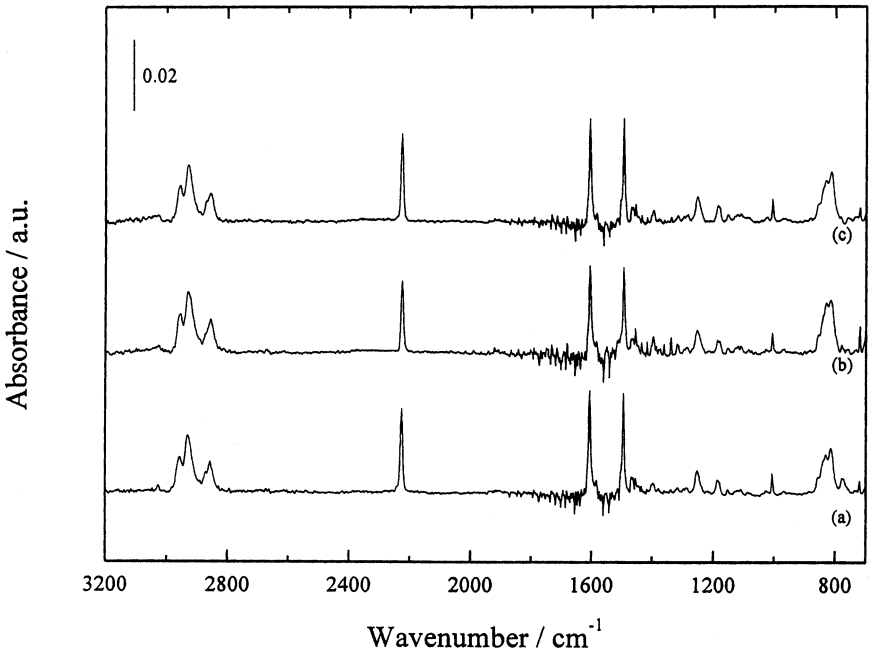

FIGURE 14 The same as in Figure 13, but for nematic 5CB at 25°C on self-assembled *trans* M-AZO11.

5CB super-cooled at 20°C [17] have shown that the ν_{CN} and ν_{CC} vibrations are polarized approximately parallel to the long molecular axis, whereas the δ_{CH} vibrations are polarized perpendicular to that axis. Therefore, these vibrations serve as good indicators of the alignment of 5CB molecules. On the other hand, the CH_2 asymmetric and symmetric stretch modes are not sensitive to the molecular alignment.

It is apparent from Figure 13 that the ν_{CN} band of 5CB on the F-AZO11 SAM is stronger in the nematic phase at 25°C than in the isotropic phase at 45°C, but the reverse is true for the δ_{CH} bands. These facts reveal that the 5CB molecules in the nematic phase are aligned with their long axes perpendicular rather than parallel to the SAM film surface. This is equally true for nematic 5CB on the AZO11 SAM (not shown here). However, the intensity changes of these bands caused by the isotropic-nematic phase transition are smaller for 5CB on the SAM of M-AZO11 as shown in Figure 14, indicating that the nematic 5CB molecules on the M-AZO11 SAM film are less ordered. We attribute this less ordering to the terminal O-CH_3 group.

Effect of Photoisomerization of *trans* AZO11 SAMs on 5CB Alignment in the Nematic Phase

In this section we deal with IRRAS spectral changes of nematic 5CB molecules on the SAMs of *trans* AZO11 derivatives caused by irradiation with UV and visible in sequence. Figures 15 and 16 depict the IRRAS spectra of 5CB films at 25°C on the SAMs of *trans*-form F-AZO11 and M-AZO11, respectively, and those observed after subsequent UV and visible irradiations. All the prominent bands observed in these figures concern the vibration modes with their transition moments approximately parallel to the long axis of 5CB molecule, as described before. In each set of the figures, (a) refers to the *trans*-form SAM, whereas (b) and (c) involve the SAMs illuminated with UV followed by visible radiation. It is clear that upon UV irradiation of the *trans* F-AZO11 SAM both the ν_{CN} and ν_{CC} bands decrease only a little in intensity; the ν_{CN} band shows a 6% decrease in intensity after *trans*-to-*cis* isomerization of the F-AZO11 SAM as in the case of AZO11 SAM (not shown here). This intensity decrease suggests a small change toward a parallel alignment of the 5CB molecules with respect to the gold surface in response to the parallel alignment of the terminal phenyl-N moiety caused by *trans*-to-*cis* isomerization of the F-AZO11 SAM. In this case the phenyl-phenyl interaction of 5CB and F-AZO11 may be considered as a primary cause of the parallel alignment.

Although the change in the alignment of 5CB due to *trans*-to-*cis* isomerization is very small as described above, UV irradiation of the *trans* M-AZO11 SAM has little influence on the intensities of the ν_{CC} and ν_{CN} bands, as shown in Figure 16. This consists perfectly with the negative evidence for the *trans*-to-*cis* isomerization of M-AZO11's SAM in Figure 10. Reasonably the subsequent visible irradiation also causes little change in the spectrum shown in Figure 16(c). One may notice in Figure 15 that the *cis*-to-*trans* isomerization of the F-AZO11's SAM leads to a little more perpendicular alignment of 5CB molecules, which probably means that distortions in the alignment were more or less removed in the reorientation process.

Effect of Photoisomerization of *cis* AZO11 SAMs on 5CB Alignment in the Nematic Phase

Figures 17–19 show the irradiation-induced IRRAS spectral changes of nematic 5CB at 25°C deposited on the SAMs of *cis*-form AZO11, F-AZO11, and M-AZO11, respectively. In each figure, (a) refers to the originally prepared *cis*-form SAM, whereas (b) and (c) refer to the SAMs subjected to visible and UV irradiations in sequence. While nematic LC molecules generally tend to align themselves parallel to their long axes, their easy direction varies dependent on the nature of the substrate surface [18]. The easy

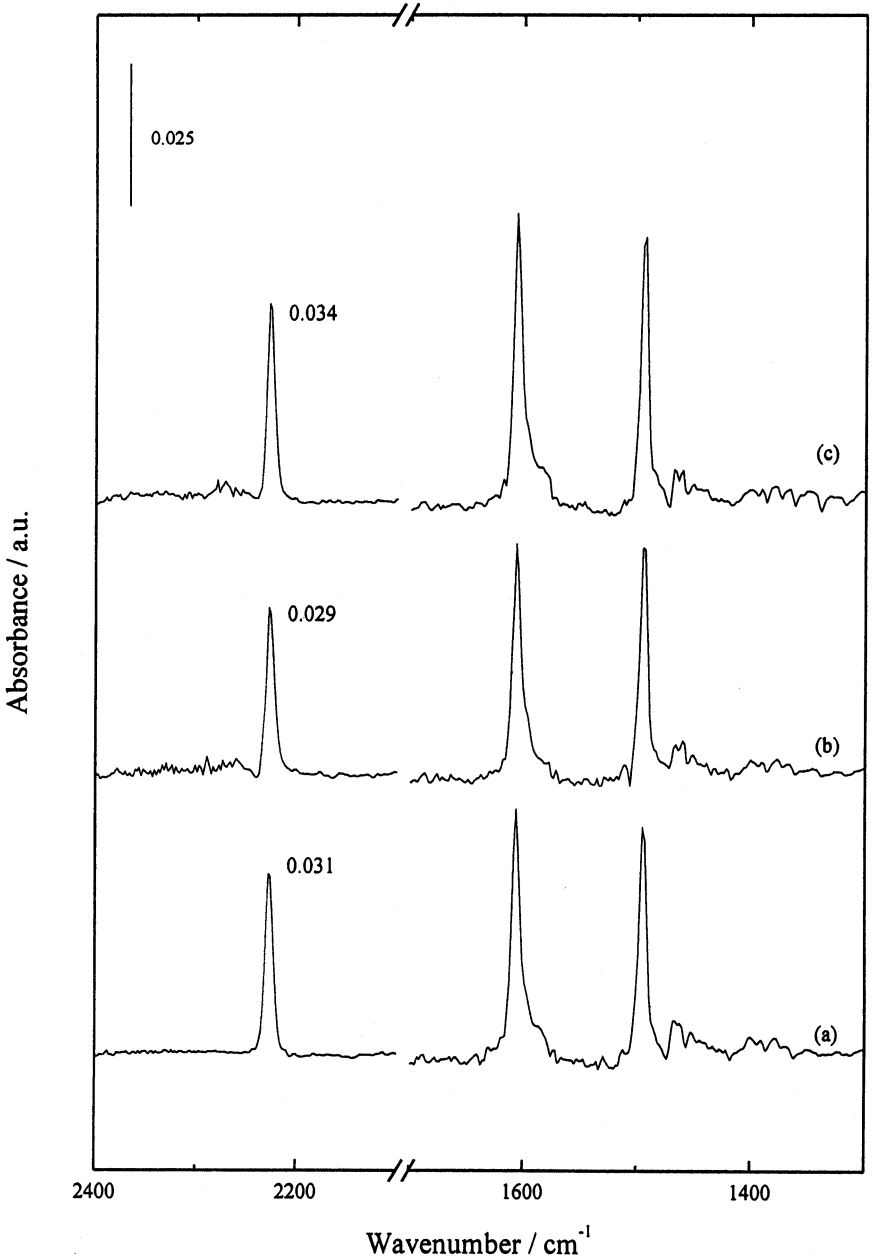

FIGURE 15 IRRAS spectral changes of 100 nm thick nematic 5CB at 25°C on self-assembled *trans* F-AZO11: (a) before UV irradiation, (b) after UV irradiation (20 min), and (c) after visible irradiation (20 min) in sequence.

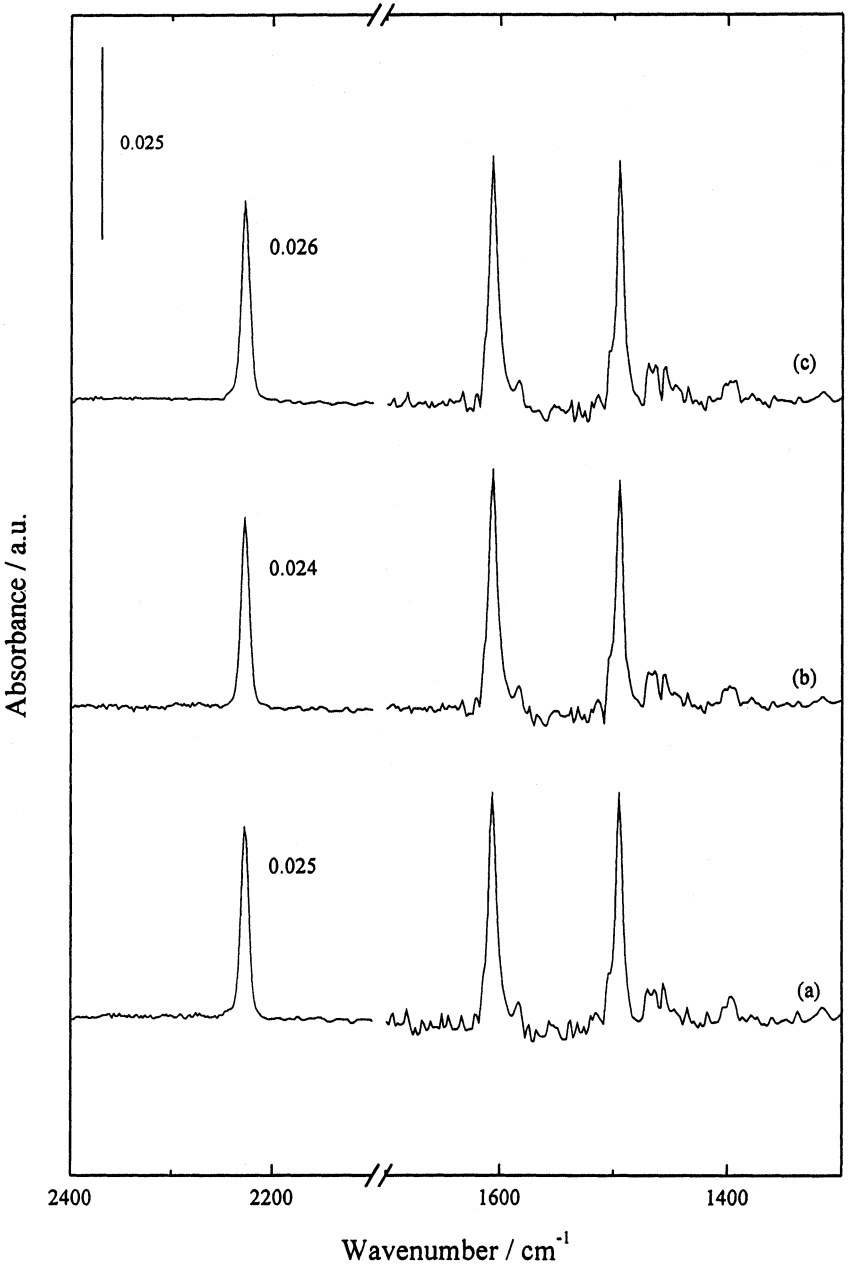

FIGURE 16 The same as in Figure 15, but for nematic 5CB at 25°C on self-assembled *trans* M-AZO11.

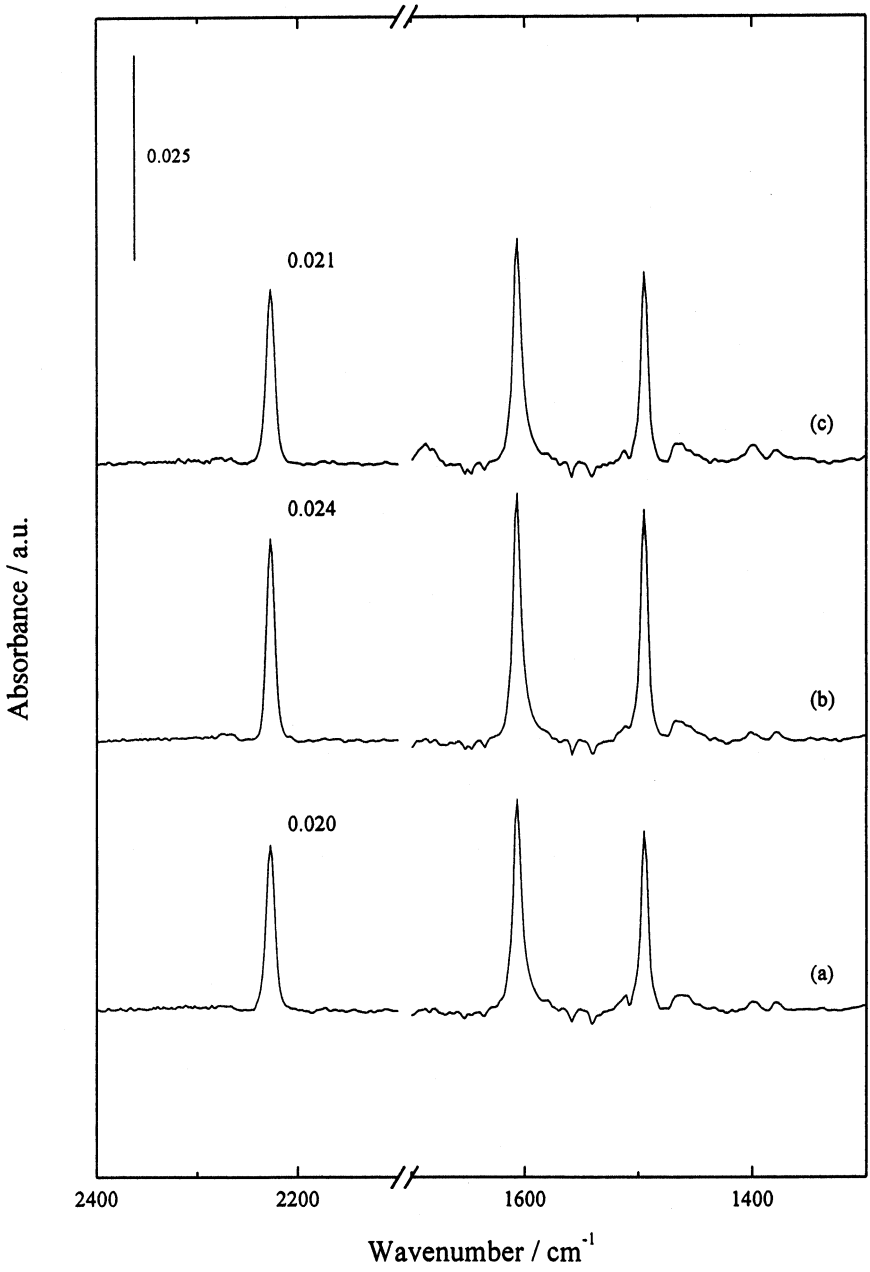

FIGURE 17 IRRAS spectral changes of 100 nm thick nematic 5CB at 25°C on self-assembled *cis* AZO11: (a) before visible irradiation, (b) after visible irradiation (20 min), and (c) after UV irradiation (20 min) in sequence.

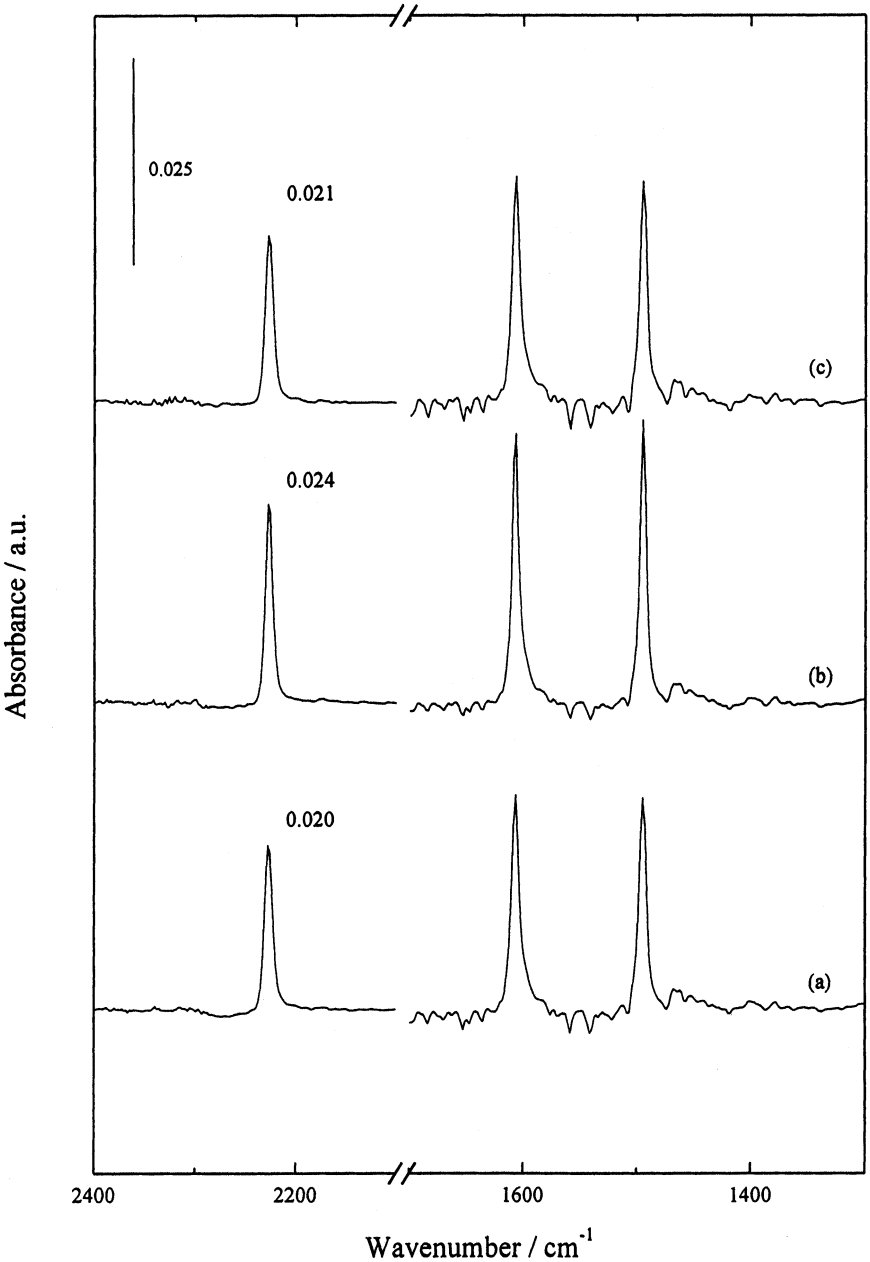

FIGURE 18 The same as in Figure 17, but for nematic 5CB at 25°C on self-assembled *cis* F-AZO11.

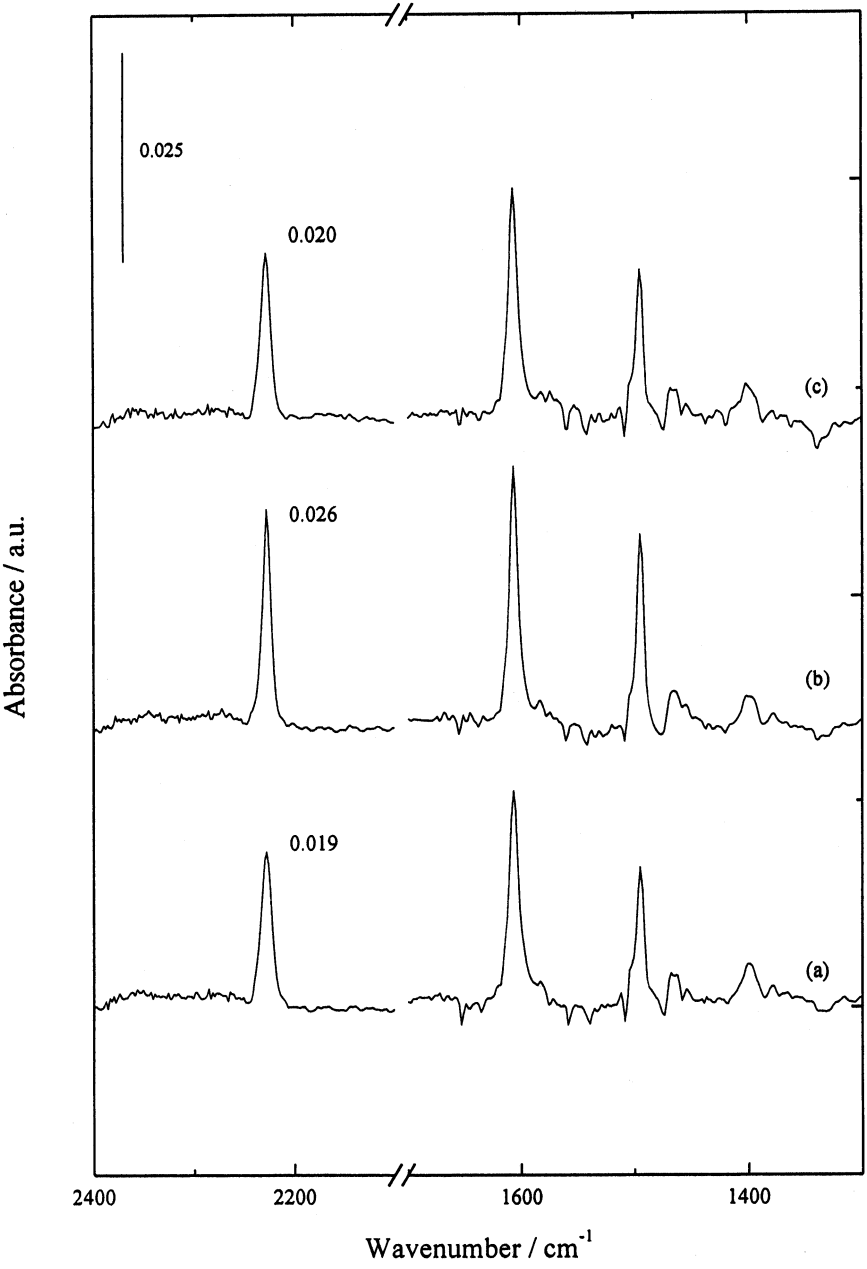

FIGURE 19 The same as in Figure 17, but for nematic 5CB at 25°C on self-assembled *cis* M-AZO11.

directions of 5CB on the SAMs of ***trans*** AZO11 derivatives are normal to the SAM film surfaces, but on the SAMS of ***cis*** AZO11 derivatives they are parallel, as mentioned previously. In addition, for each of the ***trans***-form SAMs the azobenzene group is upright on the gold surface as the long aliphatic chain so that the head of the azobenzene group (i.e., O-CH_3 for M-AZO11) in contact with 5CB would play an important role in determining the alignment of 5CB molecules. For the ***cis***-form SAMs, on the other hand, the plane of the topmost phenyl ring is bending parallel to the gold surface so that the phenyl-phenyl interactions would mostly contribute to the 5CB alignment.

From a viewpoint of the molecular cross section, a higher degree of isomerization efficiency, and in turn a larger change in the 5CB alignment, can be expected for ***cis***-form self-assembling. This indeed was observed, as shown in Figure 17, where the ν_{CN} band of 5CB on the ***cis***-form AZO11 SAM is 20% increased in intensity as a result of ***cis***-to-***trans*** isomerization. Also, the same magnitude of the intensity increase is observed for 5CB on the F-AZO11 SAM. In both cases the subsequent UV irradiation decreases the ν_{CN} band intensity to the original value, indicative of a reversible conformational change between ***trans*** and ***cis*** forms. It is noticeable that on the M-AZO11 SAM the ν_{CN} band intensity is much more increased (37%) by ***cis***-to-***trans*** isomerization, as shown in Figure 19. This is in high contrast to the case of initial assembling of ***trans*** M-AZO11, where only a small intensity change (4%) was observed (Figure 16). Thus, it is clear that the advancement of isomerization efficiency by ***cis***-form self-assembling is particularly remarkable for M-AZO11. Therefore, it seems plausible to assume that the effect of ***cis***-form assembling is larger for larger molecular cross sections.

In the above discussion we only focused on the ν_{CN} band intensity. It is seen in Figure 19 that on the ***cis*** M-AZO11 SAM the 1494 cm^{-1} band due to the ν_{CC} vibration of 5CB is much less intense than another ν_{CC} band at 1606 cm^{-1}, despite the fact that both bands are of almost compatible intensities on the ***cis*** F-AZO11 SAM (Figure 18). The same trend can also be seen on the ***cis*** AZO11 SAM (Figure 17), though not to a greater extent than on the ***cis*** M-AZO11 SAM. This is not completely understood, but we believe it may concern the fact that the transition moment of the ν_{CC} mode at 1494 cm^{-1} is directed more parallel to the molecular long axis than that of the ν_{CC} mode at 1606 cm^{-1} [17]. In this connection, it should be noted that such a difference in intensity does not occur on the originally formed ***trans*** M-AZO11 SAM that imposes a perpendicular alignment. Furthermore, for a well-ordered (i.e., uniaxially homogeneous) alignment of 5CB molecules, both ν_{CC} bands are equal in intensity [17]. Accordingly, it is likely that the intensity difference between the two ν_{CC} bands arises from some specific molecular alignment caused by the interaction with the ***cis***-form SAM surface, upon which a nonuniform planar alignment is favored.

A deep concern to the specific alignment would be the terminal O-CH_3 group of the SAM, which is pushed out of the adjoining phenyl-ring plane and could exert a steric effect; it is highly possible that the CH_3 group enfeebles the phenyl-phenyl interaction. In any event, it is quite clear that the alignment of 5CB molecules is very sensitive to the headgroup of AZO11 derivatives. This means that liquid crystal molecules can serve the purpose of molecular recognition.

CONCLUSIONS

The self-assembly of azobenzenealkanethiols on gold films and the photoisomerization of the resulting SAM films have been investigated using IRRAS spectroscopy. It was shown that the *trans*-form SAMs set limits to photoisomerization to *cis*-form SAMs, in contrast to photoisomerization in solution. This arises from larger cross-sections for the *cis* isomers than for the *trans* isomers. Indeed, we found that originally prepared *cis*-form SAMs gave relatively high degrees of *cis*-to-*trans* isomerization efficiency. The same conclusion was derived from IRRAS spectral changes due to concomitant changes in the alignment of nematic 5CB liquid crystal molecules deposited on the SAMs. From an applied point of view, the photo-induced isomerization is attractive for alignment control of liquid crystals. In order to put this control into practice, however, a more significant improvement of the photoisomerization efficiency is indispensable. Our separate investigations reveal that self-assembling of *trans* AZO11 in cooperation with shorter alkanethiol molecules is valuable.

REFERENCES

[1] Losic, D., Shapter, J. G., & Gooding, J. J. (2000). *Langmuir*, *17*, 3307.
[2] Laibinis, P. E., Whitesides, G. M., Allara, D. L., Tao, Y.-T., Parikh, A. N., & Nuzzo, R. G. (1991). *J. Am. Chem. Soc.*, *113*, 7152.
[3] Laibinis, P. E., & Whitesides, G. M. (1992). *J. Am. Chem. Soc.*, *114*, 1990.
[4] Ueda, M., Fujishima, N. Kudo, K., & Ichimura, K. (1997). *J. Mater. Chem.*, *7*, 641.
[5] Ichimura, K., Suzuki, Y., Seki, T., Hosoki, A., & Aoki, K. (1988). *Langmuir*, *4*, 1214.
[6] Ichimura, K., Hayashi, Y., Akiyama, H., & Ishizuki, N. (1993). *Langmuir*, *9*, 3298.
[7] Ichimura, K., Hayashi, Y., Akiyama, H., Ikeda, T., & Ishizuki, N. (1993). *Appl. Phys. Lett.*, *63*, 26.
[8] Maak, J., Ahuja, R. C., & Tachibana, H. (1995). *J. Phys. Chem.*, *99*, 9210.
[9] Seki, T., Fukuda, R., Yokoi, M., Maki, T., & Ichimura, K. (1996). *Bull. Chem. Soc. Jpn.*, *69*, 2375.
[10] Bell, A. T., & Hair, M. L. (Eds.). (1980). *Vibrational Spectroscopies for Adsorbed Species*. Washington, D.C: American Chemical Society.
[11] Hoffmann, F. M. (1983). *Surf. Sci. Rept.*, *3*, 103.
[12] Chabal, Y. J. (1988). *Surf. Sci. Rept.*, *8*, 211.

[13] Suëtaka, W. (1999). ***Methods of Surface Characterization, Vol 3: Surface Infrared and Raman Spectroscopy, "Methods and Applications."*** New York: Plenum.
[14] Greenler, R. G. (1966). ***J. Phys. Chem.***, ***44***, 310.
[15] Zimmerman, G., Chow, L., & Paik, U. (1957). ***J. Am. Chem. Soc.***, ***80***, 3528.
[16] Caldwell, W. B., Campbell, D. J., Chen, K., Herr, B. R., Mirkin, C. A., Malik, A., Durbin, M. K., Dutta, P., & Huang, K. G. (1995). ***J. Am. Chem. Soc.***, ***117***, 6071.
[17] Hatta, A. (1981). ***Mol. Cryst. Liq. Cryst.***, ***74***, 195.
[18] Urbach, W., Boix, M., & Guyon, E. (1974). ***Appl. Phys. Lett.***, ***25***, 479.